Chiral Resolution of Racemic Crystals

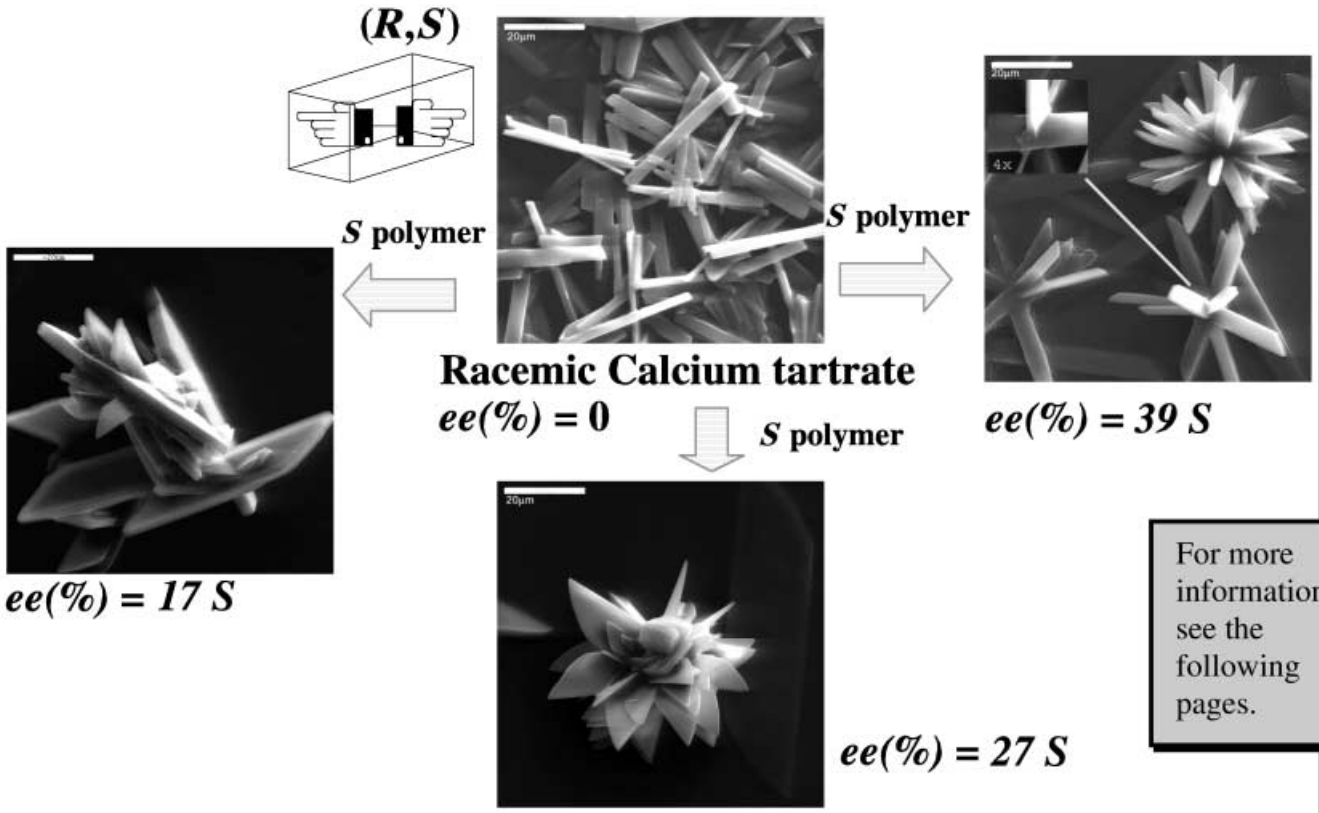

For more information see the following pages.

Stereoselective Adsorption at Crystal Surfaces

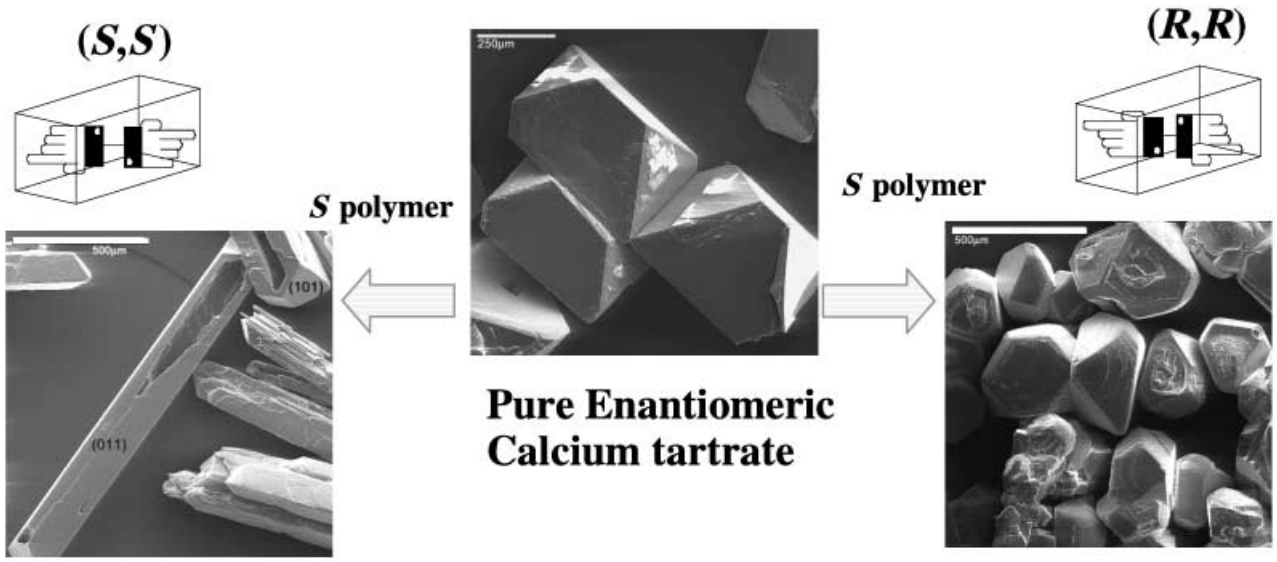

  0947-6539/02/0811-2429 $ 20.00+.50/0

The Separation of Racemic Crystals into Enantiomers by Chiral Block Copolymers

Yitzhak Mastai,*[a] Miloš Sedlák,[b] Helmut Cölfen,[a] and Markus Antonietti[a]

Abstract: A series of chiral double hydrophilic block copolymers (DHBCs) was synthesized and employed as additives in the crystallization of calcium tartrate tetrahydrate (CaT). We found that appropriate polymers can slow down the formation of the thermodynamically most stable racemic crystals as well as the formation of one of the pure enantiomeric crystals so that chiral separation by crystallization occurs even when racemic crystals can be formed. In addition, the presence of DHBCs results in major modifications of crystal morphology, creating unusual morphologies of higher complexity. Our study demonstrates the potential application of chiral DHBCs in the control of chirality throughout crystallization, in particular for racemic crystal systems, and also shows that enantiomeric excess of one enantiomer can be maximized by the kinetic control of crystallization.

Keywords: calcium · chiral resolution · crystal growth · hydrophilic block copolymers · polymers

Introduction

The discovery of the importance of stereochemistry in biochemical environments dates back to 1860 when Pasteur reported the different rates of destruction of *dextro* and *levo* ammonium tartrate by the mold *Penicillium glaucum*.[1] Since then resolution of racemic compounds has been of fundamental importance both for pure science and for applications. Among those, the resolution of racemic drugs is extremely important in view of the fact that optical isomers of drugs can exhibit different pharmacological profiles in living systems.[2] The significance of optically pure drugs is reflected in the new FDA[3] and European community[4] regulations for the approval of new chiral drugs, which demand pharmacological and toxicological tests of all drug enantiomers.

Resolution of isomers can be achieved by various processes based on physical, chemical, and biological techniques. Among them, chemical methods have a long history. For instance preferential crystallization and diastereomeric salt formation[5] have been in use for more than 100 years. In recent decades there has been a remarkable advance in the separation of enantiomers. New chromatographic techniques[6] based on the strategy of linking chiral compounds to a solid substrate and using the resultant material to selectively bind one enantiomer were developed. Not only chiral organic compounds, but also biologically derived materials such as enzymes, amino acids, sugars, and antibodies can be coupled to a solid substrate and used as the stationary phase in chiral chromatography. Although these techniques show high chiral discrimination, none of them is yet applicable for the resolution of enantiomers on a large scale; therefore large-scale separation technology is still based on the classical crystallization methods.

In recent years, new approaches to the optical resolution and purification of organic enantiomers based on chiral recognition have been employed. For instance Lahav and coworkers[7–11] developed a new general methodology, termed "tailor-made additives", for the kinetic resolution of conglomerates (mixtures of independent crystals of both enantiomers) and racemic mixtures that is in principle suitable for large-scale applications. This separation method is based on the addition of enantiospecific chiral inhibitors that prevent or delay the growth of one of the enantiomorphs. For example in the crystallization of (*R,S*)-threonine a resolving additive with stereochemical similarity to the (*R*)-threonine is employed (e.g., (*R*)-glutamic acid), and a chiral discrimination of 94.8 % of (*S*)-threonine is achieved. This process underlies the so-called "rule of reversal",[8] where an *R* additive is absorbed selectively on the growing *R* enantiomorph crystal or crystal nucleus and as a result delays the growth of the *R* crystal; consequently the enantiomorph of the opposite chirality precipitates in excess. It should be pointed out that the "tailor-made additives" method is applicable for the resolution of conglomerates and racemic systems, for instance the resolution of racemic histidine.[9] The resolution process is ration-

[a] Dr. Y. Mastai, Dr. H. Cölfen, Prof. M. Antonietti
Max Planck Institute of Colloids and Interfaces
Research Campus Golm, 14424 Postdam (Germany)
Fax: (+49) 331-567-9502
E-mail: mastai@mpikg-golm.mpg.de

[b] Prof. M. Sedlák
Department of Organic Chemistry, University of Pardubice
nám Cs.Legií 565
532 10 Pardubice (Czech Republic)

  0947-6539/02/0811-2430 $ 20.00+.50/0

alized in terms of molecular recognition, specifically the stereoselective adsorption of the additive at the surface of crystals. In further studies, Zbaida and Lahav et al.[12, 13] extended this work to soluble chiral polymers.

Although the low molecular weight additives lead to high chiral discrimination, they are still limited with respect to the molecules to be separated. Most of those methods are only applicable if the racemic compound crystallizes as a conglomerate, that is, both enantiomers form independent crystals, and a mixture of those crystals is obtained. This is, however, a rare case: as a matter of fact there are only 240 compounds known to crystallize as conglomerates.[5] All other chiral compounds crystallize as racemic crystals as the thermodynamically most stable modification, where both enantiomers are found in equal proportions in each unit cell. Here, the classical point of view holds that chiral separation by crystallization processes cannot be employed at all.

In a series of papers it was recently demonstrated that double hydrophilic block copolymers (DHBCs) with appropriate chemical functionality could selectively interact with specific crystal surfaces and influence the morphology, crystalline structure and defined superstructure formation of inorganic crystals such as calcium carbonate,[14] hydroxyapatite,[15] and barium sulfate.[16] Those block copolymers were also used in the synthesis of stable noble metal and semiconductor nanocolloids.[17, 18] DHBCs consist of one block with a functionality pattern designed to interact with the crystal surface, and another hydrophilic block that, in contrast, does not interact and only provides dissolution in the solvent water.

In this paper DHBCs are employed for the resolution of racemic solutions by crystallization. For this purpose, optically active groups that are assumed to selectively interact and stabilize one crystal enantiomer are attached as a side group to a polymer backbone with a distinct number and pattern of functionalities. The overall approach is in line with the general concept of molecular recognition at crystal interfaces, yet we expect additional advantages from the use of DHBCs. In general, DHBCs as "molecular tools" not only affect crystal surfaces by the action of the functional block, but also offer stabilization during crystal nucleation and growth and do not precipitate or agglomerate the bound crystals.[19] From a technical point of view, block copolymers as high molecular weight species can easily be separated from the crystallizing substrate, thus allowing recovery of both the polymer and the enantiomers.

The chiral block copolymers are synthesized on the base of a poly(ethylene glycol)-*block*-branched poly(ethyleneimine) (PEO-*b*-PEI) copolymer where a variety of optically active functional groups are bound to the PEI. The potential of these block copolymers to control crystal chirality is illustrated in the crystallization of one racemic and one conglomerate model crystal system, namely the classical examples of the two Pasteur tartrate salts. It will be shown that the chiral block copolymers can even be employed for the resolution of the racemic crystals (though still with low chiral purity). Beside chiral discrimination, major morphology changes with unique crystal shapes are obtained during crystallization with the chiral block copolymers.

Results and Discussion

A set of optically active DHBCs was synthesized based on one polymer backbone of PEG-*b*-PEI blocks (PEG = poly(ethylene glycol), $M = 5000\ g\,mol^{-1}$, PEI = branched poly(ethyleneimine), $M = 700\ g\,mol^{-1}$). Table 1 presents the different optically active groups of the block copolymers that were employed in this study, all of them quite common natural components such as (*S*)-ascorbate (vitamin C), (*S*)-proline, or (*R*)-gluconate. In general all polymers contained 2–3 optically active side groups in the PEI polymer chain, as is evidenced by ^1H NMR and light rotation.

Table 1. Chiral copolymers used in the crystallization of racemic CaT and conglomerate $NaNH_4T$. N = number of optically active units.[a]

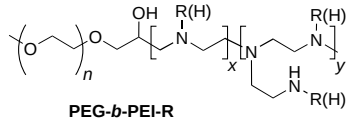

PEG-*b*-PEI-R

Block copolymer	Optically active groups R
PEG-*b*-PEI–((*S*)-proline)$_3$ $N = 3$	
PEG-*b*-PEI–((*S*)-histidine)$_3$ $N = 3$	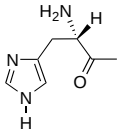
PEG-*b*-PEI–((*S*)-ascorbic acid)$_3$ $N = 3$	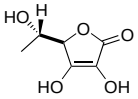
PEG-*b*-PEI–(quinine)$_2$ $N = 2$	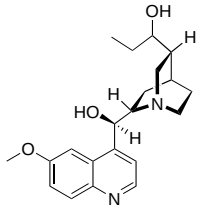
PEG-*b*-PEI–((*R*)-gluconate)$_3$ $N = 3$	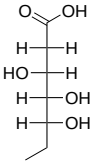

[a] PEG: polyethyleneglycol $M_W = 5000\ g\,mol^{-1}$; PEI: polyethyleneimine $M_W = 700\ g\,mol^{-1}$.

In order to demonstrate chiral discrimination by the block copolymers in the crystallization process we chose—following the very first experiments of Pasteur—sodium ammonium tartrate ($NaNH_4T$) as a model for conglomerate crystallization and calcium tartrate tetrahydrate (CaT) as a characteristic case of crystallization into a stable racemate crystal. The crystal structure of racemic CaT is not reported in the literature (although Addadi et al.[20] have studied and solved it), but the crystal structure of enantiomeric (*R,R*)- or (*S,S*)-CaT is well documented.[21–23]

  0947-6539/02/0811-2431 $ 20.00+.50/0

In Figure 1 the typical morphologies, as seen by scanning electron microscopy (SEM), of the "default" crystals (that is those without polymeric additives) are shown. The enantiomeric CaT (*R,R* or *S,S*) crystallizes as prismatic crystals (space group $P2_12_12_1$, orthorhombic unit cell), delimited by two different faces, {011} and {101} (Figure 1a). The racemate CaT crystallizes in needles with a typical length of $\approx 40\,\mu m$ (Figure 1b) and finally the $NaNH_4T$ conglomerate crystallizes in an orthorhombic structure.[24]

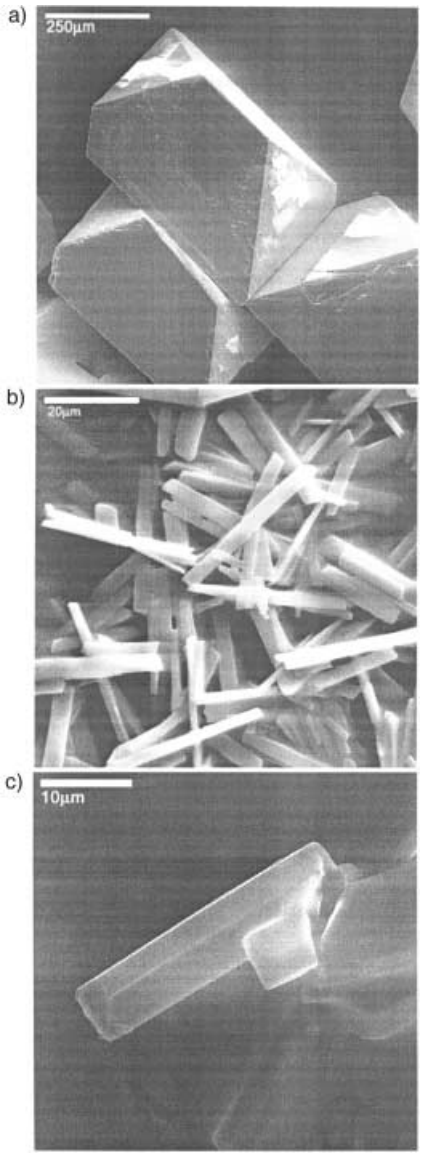

Figure 1. Scanning electron microscopy images of: a) enantiomeric (*R,R*)-calcium tartrate tetrahydrate (CaT); b) racemic CaT; c) conglomerate of sodium ammonium tartrate ($NaNH_4T$).

The presence of block copolymers as additives in the crystallization of CaT and $NaNH_4T$ results in various effects on the crystallization kinetics, crystal morphology, and chiral discrimination, which will be discussed separately. On the basis of the effects, we will differentiate between a low concentration region of 1–10 mg polymer mL^{-1} and a semi-dilute region with typical polymer concentrations of 10–30 mg polymer mL^{-1}.

Effects on crystallization kinetics: The crystallization of the $NaNH_4T$ conglomerate is relatively slow: half of the material has crystallized after 8–12 days. For each of the CaT enantiomers full crystallization is completed in two days, whereas crystallization of the racemate CaT is relatively rapid and is accomplished within a few minutes (ca. 5 min). This underlines the key problem of obtaining enantioselectivity by chiral crystallization of potential racemate crystals: one either has to slow down the formation of racemic crystals or to stimulate the formation of the pure enantiomers, and the change of kinetics has to be by more than two orders of magnitude.

In order to investigate the influence of our copolymers on the crystallization kinetics of racemate CaT, we used a calcium-ion-selective electrode, as reported in the literature for aqueous solutions and wines.[25] The calcium-ion-selective electrode measuring system has been shown to be independent of any pH effect above pH 3, and the signal output voltage is converted to calcium concentration by means of a calibration curve recorded with calcium standards. The results of the kinetic measurements in the pH region of ≈ 6.0 are shown in Figure 2.

In the presence of block copolymers the crystallization kinetics of racemate CaT is generally inhibited. For example, in a solution of 7 mg mL^{-1} PEG-*b*-PEI–(*S*)-proline, crystallization with $\approx 80\,\%$ crystal yield, as calculated from the drop in free Ca concentration, is observed after about 6 min, while without copolymers the same crystal yield is obtained in 3 min. In general, the inhibitory effect of the copolymers on the crystallization kinetics is increased as the concentration of copolymers is increased; see, for example, Figure 2D for the

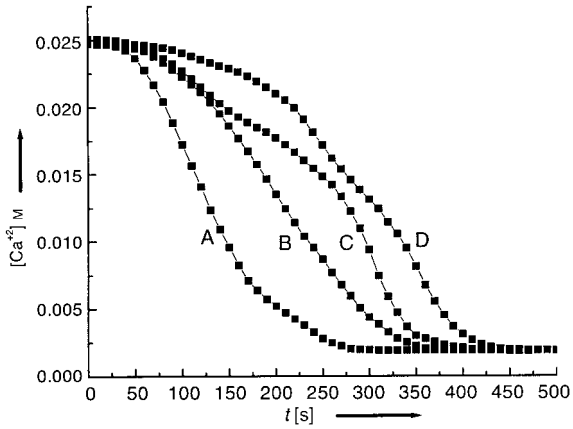

Figure 2. The kinetics of crystallization of racemic CaT in the presence of chiral copolymers. Experiments were carried out at 25 °C, pH ≈ 6.0, $[Ca^{2+}] = [\text{sodium hydrogentartrate}] = 0.025$ M. A) Pure CaT without copolymer additives. B) CaT with 5 mg mL^{-1} PEG-*b*-PEI–(*R*)-gluconate. C) CaT with 7 mg mL^{-1} PEG-*b*-PEI–(*S*)-proline. D) CaT with 25 mg mL^{-1} PEG-*b*-PEI–(*S*)-ascorbate.

case of 25 mg mL^{-1} PEG-*b*-PEI–(*S*)-ascorbate. The strongest inhibitor in this series, the PEG-*b*-PEI–quinine copolymer at high copolymer concentration (17 mg mL^{-1} and higher) retards crystallization to an overall time of 2–3 days, which is already of the right order to be considered for chiral crystallization.

0947-6539/02/0811-2432 $ 20.00+.50/0 *Chem. Eur. J.* **2002**, *8*, No. 11

For the evaluation of the kinetic effect of block copolymers on crystallization, it is meaningful to divide the kinetic data into two different regions. The first one is the crystallization induction time, which is characterized by only a small decrease in calcium concentration ($d[Ca^{2+}]/dt \approx 1 \times 10^{-3}$ mol s^{-1}); the second region is one of crystal growth, characterized by a rapid decrease in Ca concentration. It is seen that an appropriate block copolymer strongly influences the crystallization induction period, in other words, suppresses nucleation, but influences crystal growth less distinctly. For example, the induction period of pure CaT is extremely short (10–15 s) whereas the induction period in solution of 25 mg mL^{-1} PEG-*b*-PEI–(*S*)-ascorbate is ≈80 s.

It has to be pointed out that the optically active copolymers employed show practically no effect on the crystallization kinetics of each of the CaT enantiomers. The strong retardation of the racemate is in good agreement with a previous report[26] that addition of polygalacturonic acid to a model wine inhibits spontaneous precipitation of calcium tartrate. In addition, the chiral copolymers were added to standard Ca^{2+} solutions (100 mM $CaCl_2$) in order to test the potential binding of free Ca^{2+} ions. From the decrease in the calcium-selective-electrode potential, it was calculated that ≈7% of the calcium was bound by the copolymers. Therefore, the effect of ion binding to the polymers can practically be neglected. The influence on the crystallization kinetics of the $NaNH_4T$ conglomerate was not examined due to the extremely slow overall kinetics (ca. 10–12 days), which limits the use of the calcium-selective electrode.

Effects on crystal morphology: The influence of different copolymers on the morphology of racemic CaT and $NaNH_4T$ conglomerate crystals is shown in Figure 3. In the case of $NaNH_4T$ conglomerate crystals, all chiral copolymers have a similar influence on the crystal morphology, as is shown in Figure 3a. Generally addition of copolymer reduces the crystal size. For example, the average crystal size of $NaNH_4T$ precipitated from a solution of 4 mg mL^{-1} PEG-*b*-PEI–(*S*)-ascorbate is ≈20 μm, compared with ≈35 μm for the polymer-free default case. Yet the overall crystal morphology is not affected and the crystals preserve their typical shape. This suggests a nonselective influence of the chiral polymers on the conglomerate.

On the other hand, various modifications of the crystal morphology were found for the racemic CaT. Figure 3b, c depicts typical morphology modifications for low copolymer concentrations. In this concentration range, the dominant crystal morphology is rhombohedral, as compared to the typical needle-like morphology of the ordinary CaT (see Figure 1b). The degree of this transformation can be characterized by the crystal aspect ratio (*a*/*b*), which shifts from ≈40 for the ordinary CaT to ≈7 for PEG-*b*-PEI–(*R*)-gluconate-modified crystals. At semidilute copolymer concentrations, unusual crystal morphologies with higher complexity are obtained (Figure 3d, e). For example, "star"-like CaT crystals precipitated from the copolymer solution of 19 mg mL^{-1} PEG-*b*-PEI–(*S*)-ascorbate, whereas "flower"-like structures were found in 15 mg mL^{-1} PEG-*b*-PEI–(*S*)-proline. The unusual crystal shapes are not due to drying or aggregation effects, since they are also observed with light microscopy. Furthermore, high-resolution SEM of the crystals (Figure 3d inset) shows the deeply rooted growth of the crystals.

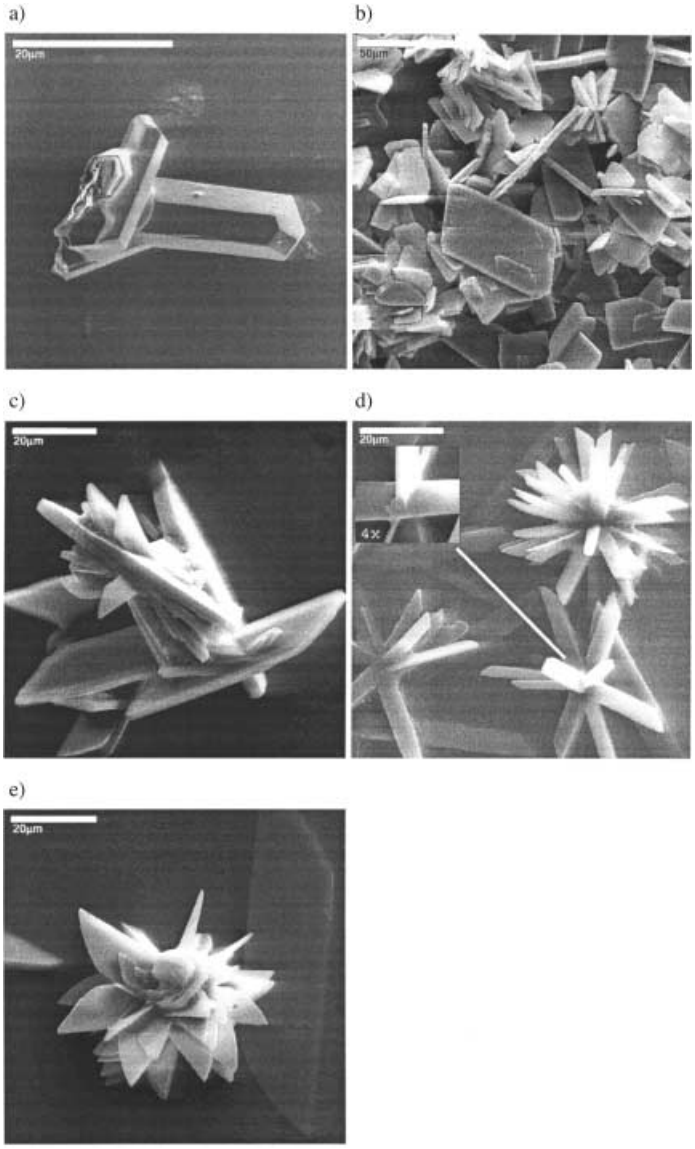

Figure 3. Crystal morphology of: a) conglomerate $NaNH_4T$ formed in the presence of 4 mg mL^{-1} PEG-*b*-PEI–(*S*)-ascorbate; b) racemic CaT formed in the presence of 7 mg mL^{-1} PEG-*b*-PEI–(*R*)-gluconate; c) racemic CaT formed in the presence of 10 mg mL^{-1} PEG-*b*-PEI–(*S*)-histidine; d) racemic CaT formed in the presence of 19 mg mL^{-1} PEG-*b*-PEI–(*S*)-ascorbate; e) racemic CaT formed in the presence of 15 mg mL^{-1} PEG-*b*-PEI–(*S*)-proline.

In a control experiment, both CaT and $NaNH_4T$ were precipitated in a solution of the parent PEG-*b*-PEI copolymer without chiral functionalities, and only a slight decrease in the crystal size (typically 10%) without any morphology modification was noticed. Hence, the chiral copolymers have a strong effect on the crystal morphology of the CaT racemic crystals, while for the $NaNH_4T$ conglomerate crystals only the size is decreased. To shed light onto the role of the polymers on the crystal morphology, which is usually explained by specific interactions of the polymers with crystal surfaces, we also examined the interaction of the different chiral copoly-

mers with the two enantiomerically pure (*R,R*)- and (*S,S*)-CaT crystals.

Figure 4 displays the crystal morphology of (*R,R*)- and (*S,S*)-CaT crystals precipitated from copolymer solutions of 10 mg mL^{-1} PEG-*b*-PEI – (*S*)-ascorbate. It can be seen that the morphology of (*R,R*)-CaT remains nearly as for the ordinary CaT while the (*S,S*)-CaT crystals show a strong orientation along the (011) plane. These results support the "rule of reversal",[8] that is the (*S*)-ascorbate interacts with the (*S,S*)-CaT; to be exact, the chiral copolymer additive interacts with enantiomorph crystals of the same chirality. The fact that the polymer modifies the growth of both the *S,S* derivative and the racemic CaT while it does not influence the growth of the *R,R* derivative is the final prerequisite of a polymer-induced racemic discrimination.

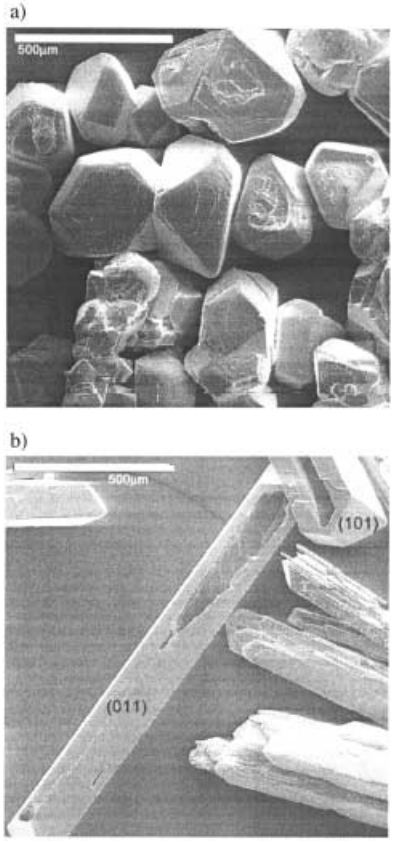

Figure 4. Crystal morphology of (*R,R*)- and (*S,S*)-CaT formed in the presence of Co-labeled 10 mg mL^{-1} PEG-*b*-PEI – (*S*)-ascorbic acid; crystal planes are marked. a) (*R,R*)-CaT; b) (*S,S*)-CaT.

Furthermore, in EDX analysis of polymer-modified *S,S* crystals produced with Co-labeled PEG-*b*-PEI – (*S*)-ascorbate (cobalt ions can complex with the amino sites of the remaining nitrogen on the polymer backbone), there is a strong Co signal (corresponding to ca. 12% Co) at the (011) plane and a relatively low Co signal (ca. 2.1%) for the plane of crystal growth (101). These results demonstrate the mode of action by a high stereochemical selectivity of copolymer adsorption at specific crystal surfaces. The (011) plane becomes exposed due to the decreased growth caused by the high polymer absorption, whereas the (101) plane has a higher surface energy, since only a small amount of polymer is adsorbed, so that it becomes the growth face.

Chiral discrimination: Before we describe the results on chiral discrimination, we should point out that CaT can crystallized only in two crystal forms, the racemic and the pure enantiomeric forms. In view of that, the chiral discrimination observed in our experiments can be interrelated to the enrichment of the pure enantiomeric crystals. The enantiopurity, namely the chiral discrimination of the DHBCs, is reported in terms of "enantiomeric excess" (*ee* %). It is speculated that the chiral discrimination exerted on the CaT racemate system is mainly due to copolymer blocking of the racemic nuclei and those of one enantiomer (with different rates) during crystallization. To confirm this assumption, we conducted time-dependent circular dichroism (CD) experiments throughout the crystallization runs.

Figure 5 shows one of these experiments. From our study of the kinetics we collected crystals at different crystallization time and from the CD peak maximum we calculated the *ee*. Analyses of the CD spectra verify high chiral discrimination in the early stages of crystallization; an *ee* of about 40% is recorded within the first few minutes of crystallization, but drops rapidly with time to the final value of ≈20%. Similar experiments in which the optical activity of the mother solution instead of the crystals was measured reveal comparable results.

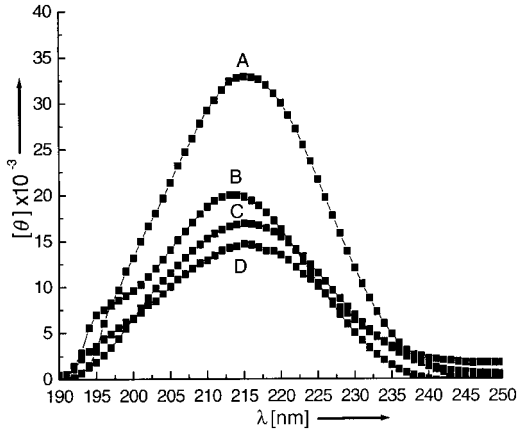

Figure 5. Time-resolved circular dichroism (CD) spectra of racemic CaT crystallization in the presence of 19 mg mL^{-1} PEG-*b*-PEI – (*S*)-ascorbate, as a function of crystallization time. A) 1.5 min, *ee* 39% *S*. B) 3 min, *ee* 25% *S*. C) 8 min, *ee* 23% *S*. D) 25 min, *ee* 19% *S* (and constant for longer experimental times, up to 3 h).

Further evidence for the generation of the metastable pure enantiomeric crystals at the expense of the thermodynamically more stable racemic crystals can be obtained from differential scanning calorimetry (DSC). The DSC curves of crystals collected at very early stages of crystallization are shown in Figure 6. Pure racemic CaT has a melting peak at 201 °C, while the DSC scan of CaT crystal collected from a polymer solution of 15 mg mL^{-1} PEG-*b*-PEI – (*S*)-ascorbate shows an additional melting peak at 178 °C, indicative for the presence of pure enantiomeric CaT crystals. DSC cannot differentiate between the presence of *R,R* and *S,S* crystals and

  0947-6539/02/0811-2434 $ 20.00+.50/0 *Chem. Eur. J.* **2002**, *8*, No. 11

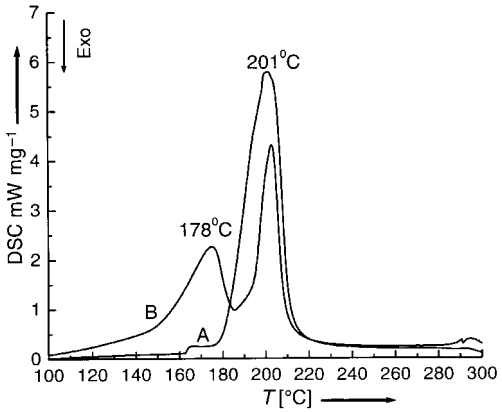

Figure 6. DSC investigations of pure racemic CaT crystals (A) and CaT crystals (B) collected from the first crystallization steps (3 min) in the polymer solution of 15 mg mL^{-1} PEG-*b*-PEI–(*S*)-ascorbate.

is therefore just taken as a measure for the suppression of the racemic crystal form.

It should be noted that similar results on chiral discrimination were obtained with the other chiral copolymers at early crystallization stages of racemic CaT; for instance, an *ee* of ≈30% is observed in a solution of 17 mg mL^{-1} of PEG-*b*-PEI–(*S*)-histidine at the early stages of crystallization, which drops to a low final *ee* value (12%). Furthermore we have to point out that the final chiral discrimination reflected in the *ee* values can fluctuate slightly upon repetition of the experiments. This relatively low fluctuation is not yet completely clear to us but appears to depend on the experimental apparatus such as glassware, dust exclusion and so on, implying possible perturbations by heterogeneous nucleation.

From these experiments it is seen that the chiral discrimination is still relatively low and accords with the kinetic behavior: the highest *ee* for CaT is found for the strongest retarder, namely PEG-*b*-PEI–(*S*)-ascorbate. In addition, the chirality of the copolymers determined the kind of enantiomer crystallized first: *S* copolymers resulted in an enantiomeric excess of *S* crystals and vice versa. Moreover, in all the cases that we examined, the chiral discrimination for the conglomerate-forming $NaNH_4T$ is by far lower than that for the racemic CaT; typical *ee* values for the conglomerate $NaNH_4T$ are 4–5%. This is in agreement with the findings reported on the effects on crystal morphology (see Figure 3), that is, that in the case of $NaNH_4T$ the polymer influences the crystal size only.

Even in spite of the rather low *ee* values, these results were significant since they demonstrated the capability of chiral block copolymers to break up the thermodynamically most stable species, the racemic crystal, and to create the metastable polymorphs, the pure enantiomer crystals, where in addition one of the two chiral versions crystallizes faster. This is an advance on the majority of previously described crystallization aids and techniques, as mainly applicable to separation of conglomerate crystals by bulk crystallization.

All these data indicate that chiral discrimination and separation is indeed a transient effect: the formation of the racemic crystal is suppressed and occurs more slowly, while first one of the enantiomers, then the other, crystallizes. This scenario points towards some possibilities for optimization: either the kinetic discrimination has to be improved (for instance by increasing the molecular weight of the binding block), or the two different effects (blocking the racemic crystal and selection of one of the enantiomers) have to be achieved by simultaneous application of two different polymers, one optimized for each task.

Beside molecular weight, the type of additive and its complementary fit to the substrate is also of key importance and was not optimized here: for example, Black et al.[27] have shown that the growth rate of {101} faces of (*S*)-asparagine monohydrate crystals is reduced to zero, that is to say completely blocked, at relatively low concentrations (5×10^{-4} M) of glutamine as an additive. The fact that application of the presented polymers also changes the shape of the crystals indicates that control of more than one crystal growth plane might also be worth considering, since the required dynamic discrimination by more than two orders of magnitude also increases the importance of less quickly growing faces of the enantiomeric crystals.

Conclusion

In the present paper, the use of double hydrophilic block copolymers with appropriate molecular functions as interactive templates in crystallization was extended to chiral copolymers and surface interactions with enantiomeric crystals. It has been shown for two model systems, CaT and $NaNH_4T$, that chiral double hydrophilic block copolymers are indeed active in chiral discrimination during crystallization of racemic crystals and conglomerates. The racemate of CaT, which usually does not form the pure enantiomorphs, was persuaded to generate 40 wt% of both enantiopure modifications and 60 wt% of the racemic crystals, as evidenced by DSC. Measurements of the optical rotation did indeed show that the enantiopure crystals were mainly composed of the *S* species, that is, the polymer suppressed not only the racemic crystal but also the *R* species. It has to be pointed out that these are two different tasks or operations needed to generate high chiral discrimination. Although the resulting enantiomeric excess is not yet very high, the basic principles of chiral discrimination by block copolymer could be demonstrated, so that future studies with optimized polymer architectures and chiral functions might result in significant improvements of the *ee*. The simultaneous employment of more than one polymer with separate functions (optimized and selected by the kinetic experiments) seems to be especially promising.

Time-dependent investigations of chiral discrimination showed high chiral discrimination at the early stages of nucleation, which dropped rapidly with crystal yield. Additionally, the presence of the DHBCs affected the crystal shape, with appearance of various unusual morphologies. This result speaks for polymer adsorption that is selective for specific crystal surfaces. The finding was also quantified by addition of cobalt salts that acted as selective contrast agents for the binding blocks of the copolymers, and differences of polymer density of up to a factor of 6 were found.

  0947-6539/02/0811-2435 $ 20.00+.50/0

Although experiments on chirality go back to the middle of the last century, knowledge in this field is still rather limited. We believe that the approach presented here using designed copolymers may provide further insight into the discrimination process. The possibility of creating block copolymers with a variety of sizes, architectures, and chemical functionalities opens new experimental opportunities for probing the pattern recognition between polymers and crystal surfaces at the molecular level.

Experimental Section

1. Synthesis of block copolymers: The optically active DHBCs used in this work were prepared by modification of PEG-*b*-PEI (PEG = poly(ethylene glycol), $M = 5000\ g\,mol^{-1}$, PEI = branched poly(ethyleneimine), $M = 700\ g\,mol^{-1}$). The synthesis of the PEG-*b*-PEI is descried in our earlier work.[28, 29] The block copolymer PEG-*b*-PEI was modified by nucleophilic reaction of amino groups with 6-bromo-6-dideoxy-(*S*)-ascorbic acid, 2,6-dideoxy-(*R*)-arabinohexonic acid, and epoxidated quinine. In the case of connection of the (*S*)-histidine and (*S*)-proline we used methods of peptide chemistry[30] to couple the amino groups of PEG-*b*-PEI to the activated carboxy group of methanesulfonic salts of the amino acids.

1.1 PEG-b-*PEI–((*S*)-ascorbic acid)$_3$ (modification of PEG*-b-*PEI by 6-bromo-6-deoxy-(*S*)-ascorbic acid)*: A solution of 6-bromo-6-deoxy-(*S*)-ascorbic acid[31] (3.85 g, 0.016 mol) in dimethoxyethane (30 mL) was added to a solution of the poly(ethylene glycol)-*block*-poly(ethyleneimine) (10 g, $M = 5700\ g\,mol^{-1}$) in dimethoxyethane (50 mL). This mixture was stirred for two days at room temperature and then the solvent was evaporated and the crude modified copolymer was purified by ultrafiltration through an AMICON membrane with MWCO (molar weight cut-off) 3000 $g\,mol^{-1}$. After lyophilization, the product was obtained as a fine brown powder (8.3 g, 77 %). $[\alpha]_D^{20} = +16.4^\circ$ ($\lambda = 230$ nm, $c = 0.8$ g in 100 mL H_2O); ^{1}H NMR (400 MHz, 25 °C, $CDCl_3$): $\delta = 1.27$ (s, 11 H; NH), 2.25 (m, 64 H; CH_2CH_2N), 3.66 (m, 440 H; CH_2CH_2O), 4.65 (m, 3 H, CH–OH); elemental analysis calcd (%) for: C 53.16, H 8.72, N 3.30; found: C 52.75, H 8.58, N 3.27; M_W calcd for: 6890 $g\,mol^{-1}$.

1.2 PEG-b-*PEI–((*S*)-histidine)$_3$ (modification of PEG*-b-*PEI by (*S*)-histidine)*: A suspension of (*S*)-histidine (2.78 g, 0.018 mol), methanesulfonic acid (3.44 g, 0.036 mol), and 1-hydroxybenzotriazole (2.42 g, 0.018 mol) in dimethylformamide (50 mL) was cooled to −15 °C. A solution of dicyclohexylcarbodiimide (3.69 g, 0.018 mol) in dimethylformamide (20 mL) was then added, and stirred at −15 °C for 30 min. A solution of poly(ethylene glycol)-*block*-poly(ethyleneimine) (10 g, $M = 5700\ g\,mol^{-1}$) in dimethylformamide (40 mL) was then added and mixed at room temperature for 3 h. The mixture was then diluted with water (80 mL), stirred for 2 h, and filtered. The filtrate was dialysed by the method described above. After final lyophilization the product was obtained as a fine white powder (8.5 g, 75 %). $[\alpha]_D^{20} = +23.1^\circ$ ($\lambda = 230$ nm, $c = 1.0$ g in 100 mL H_2O); ^{1}H NMR (400 MHz, 25 °C, $CDCl_3$): $\delta = 1.25$ (s, 4 H; NH), 2.03 (s, 11 H; NH), 2.65 (m, 64 H; CH_2CH_2N), 3.64 (m, 440 H; CH_2CH_2O), 7.05 (m, 3 H; CONH), 7.33 (s, 3 H; CH-imidazole), 7.54 (s, 3 H; CH-imidazole); elemental analysis calcd (%) for: C 48.53, H 9.06, N 4.47; found: C 49.01, H 9.11, N 4.21; M_W calcd for: 6062 $g\,mol^{-1}$.

1.3 PEG-b-*PEI–((*R*)-gluconate)$_3$ (PEG*-b-*PEI–(2,6-dideoxy-(*R*)-arabinohexonic acid)$_3$ by modification of PEG*-b-*PEI by 6-bromo-2,6-dideoxy-D-arabinohexono-1,4-lactone)*: A solution of 6-bromo-2,6-dideoxy-D-arabinohexono-1,4-lactone[32] (5 g, 0.022 mol) in dichloromethane (30 mL) was added to a solution of poly(ethylene glycol)-*block*-poly(ethyleneimine) (10 g, $M = 5700\ g\,mol^{-1}$) and triethylamine (22 g, 0.22 mol) in dichloromethane (50 mL). After refluxing overnight, the mixture was evaporated to dryness and mixed with water (50 mL). The solution of the crude modified copolymer was further purified by exhaustive dialysis against distilled water using a Spectra Pore membrane with MWCO of 1000 $g\,mol^{-1}$. After final lyophilization, the product was obtained as a fine yellowish powder (6.2 g, 57 %). $[\alpha]_D^{25} = -1.5^\circ$ ($\lambda = 240$ nm, $c = 0.175$ g in 100 mL H_2O), $[\alpha]_D^{25} = 1.1^\circ$ ($\lambda = 275$ nm, $c = 0.175$ g in 100 mL H_2O); ^{1}H NMR (400 MHz, 25 °C, $CDCl_3$): $\delta = 1.26$ (s, 11 H; NH), 2.65 (m, 64 H; CH_2CH_2N), 3.66 (m, 440 H; CH_2CH_2O), 3.91 (t, 3 H; CH–OH), 4.58 (m, 3 H; CH–OH), 4.62 (m, 3 H, CH–OH); elemental analysis calcd (%) for: C 52.80, H 9.25, N 3.16; found: C 52.56, H 9.05, N 2.72; M_W calcd for: 6190 $g\,mol^{-1}$.

1.4 PEG-b-*PEI–(quinine)$_2$ (modification of PEG*-b-*PEI by epoxyquinine)*: A mixture of quinine (5.68 g, 0.0175 mol), urea hydrogen peroxide (19.8 g, 0.21 mol), $NaHCO_3$ (1.47 g, 0.035 mol), and dicyclohexylcarbodiimide (7.22 g, 0.035 mol) in methanol (90 mL) was stirred at room temperature for 7 h.[33] Water (180 mL) was then added. After stirring for 4 h the reaction mixture was extracted by dichloromethane (4 × 80 mL). The combined organic layers were dried with Na_2SO_4 and the volume was reduced by distillation to 50 mL. The solution of poly(ethylene glycol)-*block*-poly(ethyleneimine) (10 g, $M = 5700\ g\,mol^{-1}$) as well as $BF_3 \cdot Et_2O$ (2.0 g, 0.017 mol) in dichloromethane (50 mL) was added to a prepared solution of epoxyquinine, and the mixture was refluxed overnight. After evaporation of the solvent, the crude modified polymer was dissolved in water (200 mL) and purified by ultrafiltration through an AMICON membrane with MWCO 3000 $g\,mol^{-1}$. After lyophilization, the product was obtained as fine yellow powder (8.4 g, 75 %). $[\alpha]_D^{25} = -2.1^\circ$ ($\lambda = 240$ nm, $c = 0.30$ g in 100 mL H_2O); $[\alpha]_D^{25} = +0.5^\circ$ ($\lambda = 275$ nm, $c = 0.30$ g in 100 mL H_2O); $[\alpha]_D^{25} = -0.6^\circ$ ($\lambda = 325$ nm, $c = 0.30$ g in 100 mL H_2O); ^{1}H NMR (400 MHz, 25 °C, $CDCl_3$): $\delta = 1.23$ (s, 11 H; NH), 1.59 (m, 4 H, CH_2-CH_2N), 1.75 (m, 2 H, CH-CH_2N), 2.55 (m, 70 H, CH_2CH_2N), 3.62 (m, 440 H; CH_2CH_2O), 6.14 (d, 2 H; CH-OH), 7.22 (d, 2 H, CH-arom), 7.29 (d, 2 H, CH-arom), 7.93 (d, 2 H, CH-arom), 8.61 (d, 2 H, CH=N-arom); elemental analysis calcd (%) for: C 53.42, H 9.15, N 3.82; found: C 52.24, H 9.08, N 3.19; M_W calcd for: 6350 $g\,mol^{-1}$.

1.5 PEG-b-*PEI–((*S*)-proline)$_3$ (modification of PEG*-b-*PEI by (*S*)-proline)*: A solution of (*S*)-proline (1.64 g, 0.014 mol), methanesulfonic acid (1.34 g, 0.014 mol), and 1-hydroxybenzotriazole (1.90 g, 0.014 mol) in dimethylformamide (30 mL) was cooled to −15 °C. A solution of dicyclohexylcarbodiimide (2.88 g, 0.014 mol) in dimethylformamide (20 mL) was then added, and the mixture was stirred at −15 °C for 30 min; a solution of poly(ethylene glycol)-*block*-poly(ethyleneimine) (10 g, $M = 5700\ g\,mol^{-1}$) in dimethylformamide (40 mL) was then added and mixed in at room temperature for 3 h. The mixture was then diluted with water (80 mL), stirred for 2 h, and filtered. The filtrate obtained was dialysed by the method described above. After final lyophilization the product was obtained as a fine white powder (5.8 g, 55 %). $[\alpha]_D^{25} = -3.3^\circ$ ($\lambda = 230$ nm, $c = 0.15$ g in 100 mL H_2O); $[\alpha]_D^{25} = +2.1^\circ$ ($\lambda = 300$ nm, $c = 0.15$ g in 100 mL H_2O); ^{1}H NMR (400 MHz, 25 °C, $CDCl_3$): $\delta = 1.25$ (s, 1 H, NH), 2.03 (s, 11 H, NH), 2.65 (m, 64 H; CH_2CH_2N), 3.64 (m, 440 H, CH_2CH_2O), 7.63 (t, 3 H, CONH); elemental analysis calcd (%) for: C 52.11, H 8.63, N 4.04; found: C 51.47, H 8.47, N 3.85; M_W calcd for: 5995 $g\,mol^{-1}$.

2. Crystallization experiments: All crystallization experiments were carried out at room temperature, unless noted otherwise elsewhere. The water used was purified by a MilliQ water system.

2.1 Crystallization of calcium tartrate tetrahydrate: The enantiomeric (*R,R*)- or (*S,S*)-CaT is crystallized as follows: sodium hydrogentartrate solution (50 mM, 50 mL) was mixed with $CaCl_2 \cdot 2H_2O$ (90 mM, 50 mL) at pH 6.5 and room temperature. Typically crystals of ca. 200–450 μm were formed within 1–2 days. For the crystallization of racemic CaT, identical calcium and tartrate stock solutions of 0.025 M were used. Crystallization in the presence of block copolymers was carried out as follows: first the polymers were mixed with the calcium chloride solution, then the tartrate solution was added (the final pH of the solutions was ≈6.0).

2.2 Crystallization of sodium ammonium tartrate: Crystals were grown at room temperature, in each case; aqueous ammonia was added to a solution of sodium hydrogentartrate (0.25 mM in 100 mL) with the different block copolymers, until a pH of ≈8.5 was attained. Precautions were taken in cleaning the glassware, excluding dust and so on. Crystals formed within 8–12 days; the crystals were then filtered and collected.

3. Experimental techniques: Chiral discrimination experiments were performed as follows: copolymers were added to the crystallization solutions; after complete crystallization the crystals were filtered off. Finally the specific light rotation was measured with a polarimeter (Rudolph Analytical, 589 nm, ±0.05° accuracy) by dissolving the crystals (5–10 mg) in 0.1 M HCl. A Phillips PW-1130 diffractometer was used for powder X-ray diffraction analysis. In all cases $Cu_{K\alpha}$ radiation was used. Differential thermal calorimetry analysis was carried out by means of a Netzsch TG 209 unit (Netzsch, Selb, Germany) by heating samples at a rate

  0947-6539/02/0811-2436 $ 20.00+.50/0 *Chem. Eur. J.* **2002**, *8*, No. 11

of 10 K min^{-1} up to 350 °C under argon. For the NMR experiments, a Varian Model Unity 400 operating at 400 MHz was used. Circular dichroism measurements were carried out with a JASCO CD spectrometer (Model J-715) using a cylindrical quartz cell (0.1 mL) at room temperature. Measurements of the kinetics of crystal growth of CaT were made under the same conditions as described for the crystallization experiments. A calcium-selective electrode (CSE-Orion 93) was used and an Ag/AgCl electrode served as reference. The millivolt output of the CSE is converted to calcium concentration by means of standard calibration solutions.

Acknowledgements

Financial support by the Max Planck Society is gratefully acknowledged. Y.M. acknowledges a Minerva scholarship from the Minerva Foundation. H.C. thanks the Dr. Hermann Schnell Foundation for financial support. M.S. is grateful to Prof. K. Kefurt from the Institute of Chemical Technology Prague, for valuable discussions about sugar chemistry.

[1] L. Pasteur, *Rev. Mol. Asym*. **1860**.
[2] B. Testa, *Trends Pharmacol. Sci.* **1986**, *7*, 60–64.
[3] The FDA's policy statement for the development of new stereoisomeric drugs, *Chirality* **1992**, *4*, 338–340.
[4] The rules governing medicinal products in the European Union: *Guidelines on the Quality, Safety and Efficacy of Medicinal Products for Human Use, Vol. III, Part 2*, Office for Official Publications of the European Communities, Luxembourg, **1991**. (Also available from the DGIII website: http://dg3.eudra.org/.)
[5] J. Jacques, A. Collet, S. H. Wilen, *Enantiomers, Racemates and Resolutions*, Wiley, New York, **1981**.
[6] *Encyclopedia of Separation Science, Vol. 5* (Ed.: I. D. Wilson), **2000**, pp. 2287–2426.
[7] L. Addadi, Z. Berkovitchyellin, N. Domb, E. Gati, M. Lahav, L. Leiserowitz, *Nature* **1982**, *296*, 21–26.
[8] L. Addadi, S. Weinstein, E. Gati, I. Weissbuch, M. Lahav, *J. Am. Chem. Soc.* **1982**, *104*, 4610–4617.
[9] I. Weissbuch, A. D. Zbaid, L. Addadi, L. Leiserowitz, M. Lahav, *J. Am. Chem. Soc*. **1987**, *109*, 1869–1871.
[10] I. Weissbuch, R. Popovitz-Biro, L. Leiserowitz, M. Lahav, in "*The Lock-and-Key Principle*" (Ed.: J. P. Behr), Wiley, **1995**, pp. 173–247.
[11] I. Kuzmenko, I. Weissbuch, E. Gurovich, L. Leiserowitz, M. Lahav, *Chirality* **1998**, *10*, 415–424.
[12] D. Zbaida, I. Weissbuch, E. Shavitgati, L. Addadi, L. Leiserowitz, M. Lahav, *React. Polym.* **1987**, *6*, 241–253.
[13] D. Zbaida, M. Lahav, K. Drauz, G. Knaup, M. Kottenhahn, *Tetrahedron* **2000**, *56*, 6645–6649.
[14] H. Cölfen, M. Antonietti, *Langmuir* **1998**, *14*, 582–589.
[15] M. Antonietti, M. Breulmann, C. G. Göltner, H. Cölfen, K. K. W. Wong, D. Walsh, S. Mann, *Chem. Eur. J.* **1998**, *4*, 2493–2500.
[16] L. Qi, H. Cölfen, M. Antonietti, *Angew. Chem*. **2000**, *112*, 617–621; *Angew. Chem. Int. Ed.* **2000**, *39*, 604–607.
[17] S. N. Sidorov, L. M. Bronstein, P. M. Valetsky, J. Hartmann, H. Cölfen, H. Schnablegger, M. Antonietti, *J. Colloid. Interf. Sci*. **1999**, *212*, 197–211.
[18] L. Qi, H. Cölfen, M. Antonietti, *Nano Letters* **2001**, *1*, 61–65.
[19] H. Cölfen, *Macromol. Rapid Commun*. **2001**, *22*, 219–252.
[20] F. Frolow, E. Zimmerman, L. Addadi, unpublished results.
[21] F. C. Hawthorne, I. Borys, R. B. Ferguson, *Acta Crystallogr. B* **1982**, *38*, 2461–2463.
[22] R. Boese, O. Heinemann, *Z. Kristallographie* **1993**, *205*, 348–349.
[23] G. K. Ambady, *Acta Crystallogr. Sect. B* **1968**, *24*, 1548.
[24] Z. Brozek, K. Stadnicka, *Acta Crystallogr. Sect. B* **1994**, *50*, 59–68.
[25] A. J. McKinnon, G. R. Scollary, D. H. Solomon, P. J. Williams, *Colloid Surf. A* **1994**, *82*, 225–235.
[26] A. J. McKinnon, P. J. Williams, R. S. Geoffrey, *J. Agric. Food Chem*. **1996**, *44*, 1382–1386.
[27] S. N. Black, R. J. Davey, M. Halcrow, *J. Cryst. Growth* **1986**, *79*, 765–774.
[28] M. Sedlak, M. Antonietti, H. Cölfen, *Macromol. Chem. Phys.* **1998**, *199*, 247–254.
[29] M. Sedlak, H. Cölfen, *Macromol. Chem. Phys.* **2001**, *202*, 587–597.
[30] G. C. Windridge, E. C. Jorgensen, *J. Am. Chem. Soc.* **1971**, *93*, 6318–6319.
[31] K. Bock, I. Lundt, C. Pedersen, *Carbohydr. Res.* **1979**, *68*, 313–319.
[32] K. Bock, I. Lundt, C. Pedersen, *Acta Chem. Scand. Ser. B* **1984**, *38*, 555–561.
[33] R. W. Murray, K. Iyanar, *J. Org. Chem.* **1998**, *63*, 1730–1731.

Received: November 16, 2001 [F3695]